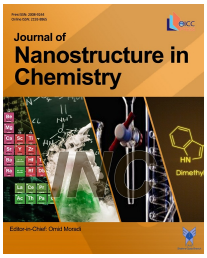

Volume 15, Issue 2, 152508 (1-14)

Journal of Nanostructure in Chemistry (JNSC)

https://doi.org/10.57647/jnsc.2025.1502.08

Amphiphilic Graphene Quantum Dots and Their Application in the Dispersion of Graphite

Zahra Azimi, Beheshteh Sohrabi*, Yasaman Javanmard, Armin Hajipour Keyvani

Department of Physical Chemistry, Faculty of Chemistry, Surface Chemistry Research Laboratory, Iran University of Science and Technology, Tehran, 16846-13114, Iran.

***Corresponding author:** sohrabi_b@iust.ac.ir

Original Research

Received:
9 March 2025

Revised:
29 March 2025

Accepted:
25 April 2025

Published online:
30 April 2025

Abstract:

One of the most auspicious and economically sound techniques for generating graphene is recognized as liquid-phase exfoliation (LPE). This empirical investigation has astutely show cased that by functionalizing hydrophilic graphene quantum dots (OH-GQDs) with hydrophobic tridecylamine, an effortlessly devised synthesis approach can be formulated, thereby producing alluringly versatile amphiphilic GQDs. This research aimed to generate a series of graphene quantum dots (GQDs) with varying amine values and employ these nanomaterials to disintegrate and distribute pure graphite in water. Adjacent graphene sheets and the GQDs on the graphene surface exhibit attractive van der Waals forces, generating a steric repulsion between them. Based on our research results, it has been found that tridecyl amine functionalized graphene quantum dots (t-GQDs) exhibit the highest ability to stabilize graphene at a greater extent compared to other functional groups. Notably, the graphene concentration peaked when t-GQDs were functionalized at a molar ratio of Amine/Citric acid = 1. Furthermore, we also explored the impact of varying concentrations of amphiphilic GQDs on the yield and dimensions of graphene nanosheets.

This study compared the stabilization effects of t-GQDs with those of several other functional groups, including amine, carboxyl, and hydroxyl groups. The comparison was based on the degree of graphene dispersion achieved, evaluated through UV-visible spectroscopy, and the stability of the dispersions indicated by zeta potential measurements. Our results showed that t-GQDs provided superior stabilization due to the optimal balance of hydrophobic and hydrophilic functionalities, which enhanced both steric and electrostatic stabilization mechanisms.

Keywords: Liquid phase exfoliation; Graphene quantum dot; Aqueous dispersion, High-power sonication; Amphiphilicity

Cite this article: Azimi, A., Sohrabi, B., Javanmard, Y., Hajipour Keyvani, A. Amphiphilic Graphene Quantum Dots and Their Application in the Dispersion of Graphite. *J Nanostruct Chem* **15**(2), Article 8 (2025).

1. Introduction

Carbon, a highly prevalent element globally, occurs in various forms called allotropes [1]. In 2004, during their research endeavor, Novoslov et al. unveiled graphene as a two-dimensional carbon allotrope [2]. As per their findings, this groundbreaking substance is anticipated to possess many exceptional attributes, such as remarkable thermal conductivity, mechanical rigidity, fracture resistance, and extraordinary electrical mobility, owing to its excellent carrier transport behavior [3]. Numerous approaches have been proposed so far to produce graphene. These methods can generally be classified into two main categories: bottom-up and top-down procedures [4]. Among them, liquid-phase exfoliation (LPE) has emerged as a promising and cost-effective technique for graphene production [5, 6]. To achieve exfoliation, considerable energy is required to overcome the van der Waals forces that hold graphite layers together. However, there is a potential solution to exfoliate graphite effectively within liquid environments by utilizing ultrasound to extract individual layers of the material [7]. Although graphene has low surface energy, it cannot disperse in water due to the high surface tension of water. However, it has been discovered that adding amphiphilic dispersing agents can prevent graphene sheets from restacking by creating electrostatic or steric repulsion between them [8]. In the case of graphite and graphene, which are highly hydrophobic, the use of surfactants or hydrophilic organic

molecules becomes necessary to disperse them in water, as these substances possess hydrophobic solid properties [9, 10]. Increasing the length of the surfactant chains leads to an increase in the dispersibility of nanosheets. This is attributed to the greater hydrophobicity of longer surfactant chains [11]. Surfactants play a crucial role during exfoliation by stabilizing the nanosheets and preventing their reaggregation.

Introducing surfactants to water reduces its surface tension to match that of graphene, making exfoliation possible. Extensive simulations and experimentation have demonstrated that organic solvents with surface energies similar to graphene are more effective in dispersing graphene than solvents with significantly different surface energies, such as NMP, DMF, and DMSO [12]. Graphene quantum dots (GQDs), derived from graphite at the nanometer scale, have gained significant attention in research due to their remarkable mechanical, optical, and electronic properties [13, 14]. These GQDs are synthesized through a bottom-up approach involving a series of chemical reactions using techniques such as pyrolysis [15], carbonization [16], and stepwise organic synthesis [17]. It has been observed that the amphiphilic nature of GQDs is an attractive feature, leading to their recent application in dispersing and exfoliating graphene nanosheets (GNs) through liquid phase exfoliation (LPE) in an aqueous medium, thanks to their amphiphilicity [18–20]. Substantial evidence supports the idea that functional hydrophilic groups on GQDs can ionize in water, enhancing their solubility and enabling effective dispersion of hydrophobic graphene sheets [21, 22]. Furthermore, the aromatic cores of GQDs contribute to the stability of graphene dispersion when combined with suitable functional groups [23].

Conventional GQDs synthesized via oxidative or hydrothermal cutting of graphene oxide sheets typically contain only hydrophilic groups such as –COOH or –OH and are thus non-amphiphilic. These GQDs, while dispersible in aqueous media, generally lack the interfacial activity required to effectively interact with hydrophobic surfaces like pristine graphene. For example, Pan et al. [24], synthesized blue-emitting GQDs by hydrothermal cutting of graphene oxide, which showed excellent photoluminescence properties but were not amphiphilic and hence not suitable as dispersants for hydrophobic materials. Their lack of hydrophobic domains restricts their ability to stabilize graphene dispersions, which require both $\pi-\pi$ stacking affinity and amphiphilic balance to overcome van der Waals-induced aggregation. In contrast, our amine-functionalized GQDs exhibit amphiphilic character, possessing both hydrophilic amine groups and hydrophobic sp^2-carbon domains. This duality allows them to interact simultaneously with graphene surfaces and aqueous environments, significantly enhancing dispersion efficiency. Traditional surfactants such as SDS or CTAB are widely employed for dispersing hydrophobic nanomaterials. These surfactants function via micelle formation and hydrophobic tail interactions, and their performance strongly depends on achieving concentrations above the critical micelle concentration (CMC). Additionally, their interactions with graphene are largely non-specific and reversible, often resulting in relatively poor long-term stability.

Amphiphilic GQDs offer a fundamentally different mechanism of dispersion. As shown by Lu et al. [25], amphiphilic GQDs can act as a new class of surfactants due to their combined hydrophilic and hydrophobic domains along with strong $\pi-\pi$ interactions. These structural features enable them to adsorb more strongly onto graphene surfaces and to stabilize dispersions without the need for micelle formation or high concentrations. Furthermore, they exhibit superior stability under a broader range of environmental conditions. This unique synergy was also demonstrated by Xua et al. [26], who reported that amphiphilic GQDs could be used as practical surfactants in the synthesis of fluorescent polymer microspheres, outperforming conventional surfactants in interfacial activity and colloidal stability.

This study presents a simple method for synthesizing tridecylamine functionalized GQDs (t-GQDs) through thermal pyrolysis of citric acid and tridecylamine. A range of GQDs with varying amine values were successfully produced, then utilized as exfoliation and dispersion agents for pristine graphene in water. The amphiphilic nature of these t-GQDs allows them to adsorb onto graphite surfaces via their conjugated aromatic rings, facilitating interaction with the surface. The synthesis method employed in this study results in t-GQDs with excellent surface activity, making them ideal for preparing graphene by using them as dispersants in aqueous solutions. Our synthesis method significantly advances over traditional approaches to creating amphiphilic GQDs. While conventional methods often require multiple steps, toxic reagents, and complex purification procedures, our one-pot hydrothermal method uses environmentally friendly precursors. It achieves high functionalization efficiency in a single step. The direct condensation of citric acid with tridecylamine allows precise control over the degree of functionalization, enabling the creation of GQDs with tailored amphiphilicity. This approach simplifies the synthesis process and enhances reproducibility and scalability, making it particularly suitable for large-scale production of functionalized GQDs for graphene exfoliation applications.

2. Materials and methods

2.1 Materials

The chemicals utilized in all the experiments conducted were procured from Merck. These chemicals include citric acid ($\geq$ 99.5%), tridecylamine (98%), ammonium hydroxide solution (25%), sodium hydroxide, calcium acetate ($\geq$ 99%), hydrochloric acid (37%), and graphite powder (Product Number 332461, $<$ 20 μm). Deionized water with the resistivity of 18.2 MΩ·cm was employed for the experiments. All chemicals were used as received without further purification.

2.2 Preparation of surface-modified GQDs

T-GQDs were synthesized by directly condensing and pyrolyzing citric acid, tridecyl amine, and ammonium hydroxide solution. The standard synthesis procedure involved dissolving citric acid (0.1 g), tridecylamine (0.03 g), and

ammonium hydroxide (0.04 mL) in pure water (10 mL). The resulting mixture was then transferred to a 20 mL Teflon autoclave and heated at 180 °C for 3 hours. Afterward, the autoclave was cooled to room temperature. It was necessary to adjust the pH of the solution to 7.0 by adding NaOH (0.1 M). The resulting t-GQDs were further dried using freeze-drying to obtain the final output product (Scheme 1). The synthesis method was repeated four times, with each iteration using a different amount of amine (0.01, 0.03, 0.06, 0.1 g) and labeled as t-GQDs1, t-GQDs2, t-GQDs3, and t-GQDs4, respectively.

According to a method mentioned in a published study [27], hydrophilic graphene quantum dots (OH-GQDs) were synthesized. The procedure involved the preparation of GQDs by placing 2 g of calcium acetate into a 5 mL beaker and heating it to 200 °C using a heating mantle. Within approximately 5 minutes, the calcium acetate began to liquefy. Furthermore, after 30 minutes, the transparent liquid gradually changed in color from colorless to light yellow and finally to orange, indicating the successful formation of GQDs based on the observed color transformation. To adjust the solution's acidity to pH 7.0, NaOH was added to the solution.

2.3 Dispersion of graphite

As per our research findings, functionalized graphene quantum dots (GQDs) have demonstrated potential as dispersants. In each experimental run, 50 mg of graphite powder was combined with 15 mL of aqueous solutions of (t–GQDs1), (t-GQDs2), (t-GQDs3), and (t-GQDs4), each at varying concentrations. The aim was to achieve a homogeneous colloidal solution, hence subjecting the mixture to sonication for 30 minutes at room temperature (the ultrasound time parameter was modified to observe its impact, as described in Scheme 2). During the exfoliation process, an ice bath was employed to prevent any rise in temperature within the sonication slurry. The next step involved centrifuging the solution at 5000 rpm for 15 minutes to eliminate larger graphene flakes. The resulting supernatant, which contained few-layer graphene flakes, was collected as the final graphene dispersion. To evaluate the performance of the dispersants, we obtained the supernatant from each sample and analyzed its absorption using a UV-visible light spectrophotometer. This allowed us to determine the highest graphene yield for a given concentration of each solution.

2.4 Characterization

The chemical structure and surface functional groups of GQDs were assessed employing Fourier transform infrared spectroscopy (FTIR) with a PERKIN ELMER 1720-X FTIR spectrometer. Transmission electron microscopy (TEM) images were captured using a Philips EM208, while field emission scanning electron microscopy (FE-SEM) images were obtained using a Hitachi S4800 at an accelerating voltage of 10 kV. UV-vis spectroscopy was conducted using a Shimadzu 2250, 220 UV-vis spectrophotometers. Fluorescence spectra were recorded on a fluorescence spectrometer (LS45, PerkinElmer, UK). Fluorescence spectra were recorded at multiple excitation wavelengths (320, 340, 360, and 380 nm) to investigate excitation-dependent emission properties characteristic of GQDs. All photoluminescence spectra were corrected for light scattering using appropriate baseline corrections. The surface wettability of the samples was determined through Contact angle measurements using a TY-WB47 instrument, while their contact angles were calculated using the Digimizer application. The surface tension of the surfactants was investigated using the ring method employing a Sigma 700 instrument. XRD spectrum analysis was performed using a Bruker D8 Advance diffractometer. Zeta potential measurements were carried

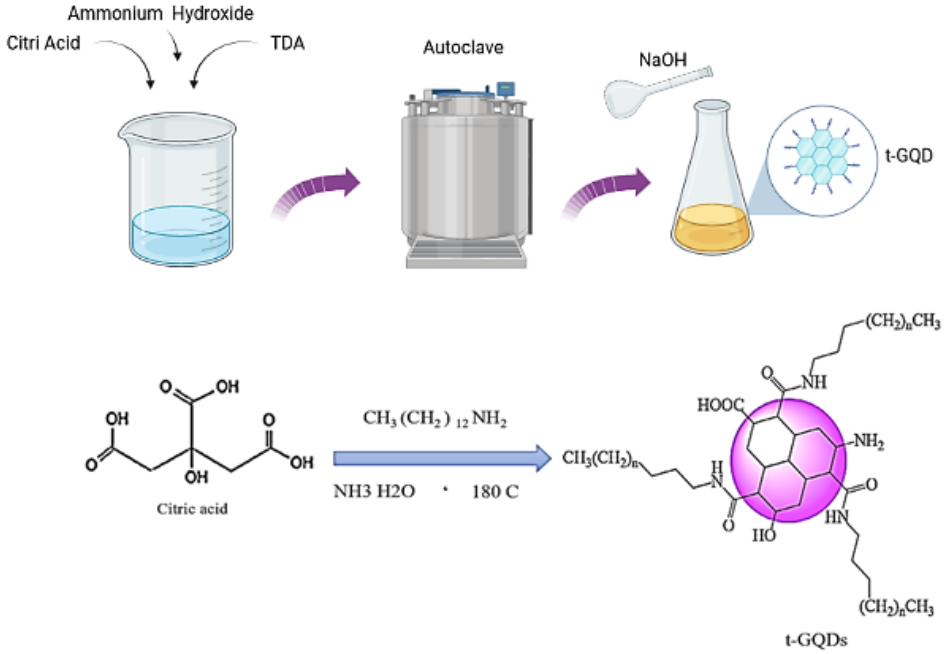

Scheme 1. The schematic diagram for the preparation of amphiphilic GQDs.

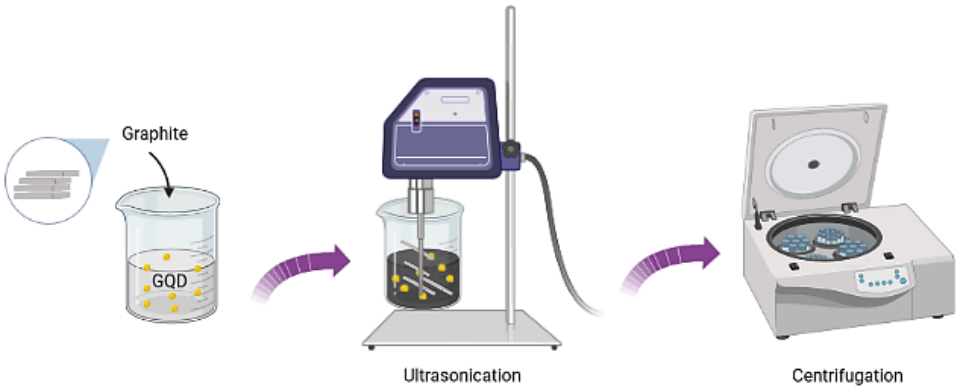

Scheme 2. Preparation process for graphene dispersion.

out using Dynamic Light Scattering (NANO-flex 180).

3. Results and discussion

Citric acid (CA) served as the sole carbon source for synthesizing OH-GQD, with its oxygenated functionalities contributing to the hydrophilicity exhibited by the resulting OH-GQDs. To achieve amphiphilicity, the introduction of hydrophobic tridecylamine became necessary. The GQDs were chemically functionalized with chain alkyl groups (tridecyl amine) through simple reactions. A hydrothermal method combined CA and ammonium hydroxide to synthesize t-GQDs. During the carbonization process, CA was transformed into GQDs. At the same time, the amine molecules reacted with the carboxyl and carbonyl groups at the GQDs' edges, thereby conferring amine functionality to t-GQDs.

FTIR spectroscopy was employed to examine the functional groups of the prepared GQDs. The presence of carboxylic acid groups at the edges of the GQDs led to the stretching vibration of C=O at 1720 cm^{-1}, as indicated by the OH-GQDs. In Fig. 1, the OH-GQDs displayed a broad absorption peak around 3434 cm^{-1}, which can be attributed to the stretching vibration of the OH bond. The carboxylic acid groups at the GQD edges also resulted in peaks at 1610 cm^{-1} and 1712 cm^{-1}, corresponding to the stretching vibrations of C=C and C=O, respectively. Furthermore, there was an absorption peak at 1406 cm^{-1}, signifying the presence of C-O, and a peak at 1242 cm^{-1}, indicating the presence of C-OH. Subsequently, following the surface modification of GQDs with amine, new peaks (amides and alkyl chains) were observed. Compared to OH-GQDs, the presence of methylene groups is indicated by the firm peaks observed at 2840 cm^{-1} and 2912 cm^{-1} in t-GQDs. This finding supports the notion that t-GQDs contain hydrophobic hydrocarbon chains. The weak absorption peak at 1427 cm^{-1} can be attributed to the stretching vibration of the C-N bond, indicating that the reaction introduces some amine groups into GQDs. The absorption peak at 1692 cm^{-1} can be ascribed to the C=O group. Moreover, the peak observed at 3595 cm^{-1} suggests the presence of NH_2 bonding, which overlaps with OH bonding [23].

The wettability of GQDs and functionalized GQDs was investigated using contact angle measurements, as shown in Fig. 2. The glass substrate was coated with synthesized OH-GQDs and t-GQDs. The contact angle of water on OH-GQDs was determined to be 5.6°, indicating high hydrophilicity. In contrast, the contact angle was altered to 33° for t-GQDs, implying a decrease in hydrophilicity. Consequently, amine functionalization was applied to the GQDs to reduce the hydrophilicity of t-GQDs. We conducted comprehensive wettability and surface activity analyses to demonstrate the amphiphilic character of our synthesized t-GQDs. The coexistence of hydrophilic carboxyl/hydroxyl groups and hydrophobic alkyl chains from tridecylamine in t-GQDs creates an actual amphiphilic structure, which we confirmed through contact angle measurements, surface tension analysis, and dispersibility tests in both polar and non-polar media.

The significant difference in contact angles between OH-GQDs (5.6°) and t-GQDs (33°) provides clear evidence of the successful incorporation of hydrophobic tridecylamine chains onto the GQD surface. While the t-GQDs maintain sufficient hydrophilicity due to remaining oxygen-containing functional groups (as confirmed by FTIR), the increase in contact angle demonstrates the introduction of hydrophobic character, confirming the amphiphilic nature of the synthesized t-GQDs.

According to Fig. 3, The surface tension measurements provide further compelling evidence of the amphiphilic character of t-GQDs. Unlike purely hydrophilic OH-GQDs, which exhibit negligible surface activity (maintaining surface tension near that of pure water), the t-GQDs significantly reduce the surface tension of water from 72.32 mN/m to 57.27 mN/m. This remarkable surface activity can only be attributed to the classical amphiphilic behavior, where the hydrophobic portions (tridecyl chains) extend into the air phase while hydrophilic portions remain in the aqueous phase, reducing interfacial energy. This behavior is consistent with conventional surfactants and confirms the successful creation of amphiphilic GQDs [28].

X-ray diffraction (XRD) analysis was utilized to investigate the structural characteristics of Graphene Quantum Dots (GQDs). As shown in Fig. 4, the obtained XRD profiles demonstrate typical patterns for both OH-GQDs and t-GQDs. In the case of GQDs, broad peaks are observed at approximately 24.4 and 23.8 degrees for (002) reflections, indicating the occurrence of graphite structures due to the

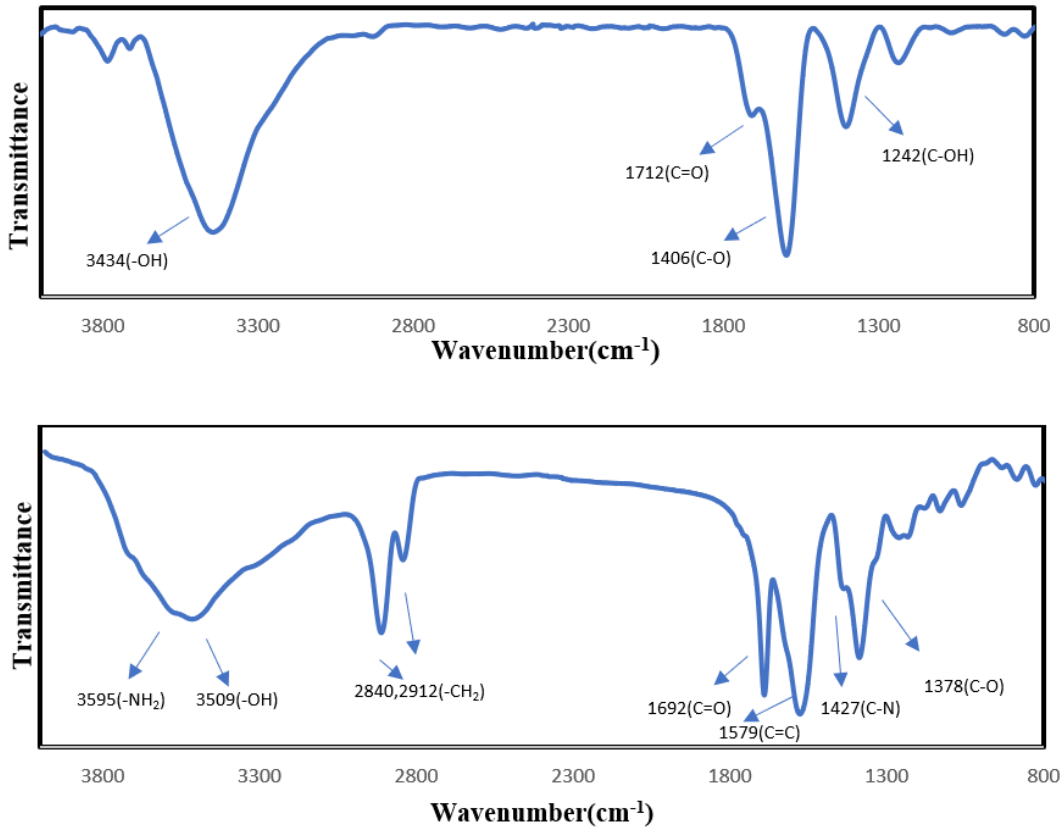

Figure 1. FTIR spectra of (a) t-GQDs and (b) OH-GQDs. Spectra were collected on KBr pellets with 1% sample loading at a resolution of 4 cm^{-1}. The wettability of GQDs and functionalized GQDs was investigated using contact angle measurements, as shown in figure 2. The glass substrate was coated with synthesized OH-GQDs and t-GQDs. The contact angle of water on OH-GQDs was determined to be 5.6°, indicating high hydrophilicity. In contrast, the contact angle was altered to 33° for t-GQDs, implying a decrease in hydrophilicity. Consequently, amine functionalization was applied to the GQDs to reduce the hydrophilicity of t-GQDs. We conducted comprehensive wettability and surface activity analyses to demonstrate the amphiphilic character of our synthesized t-GQDs. The coexistence of hydrophilic carboxyl/hydroxyl groups and hydrophobic alkyl chains from tridecylamine in t-GQDs creates an actual amphiphilic structure, which we confirmed through contact angle measurements, surface tension analysis, and dispersibility tests in both polar and non-polar media.

carbonization of CA [29]. A noticeable differentiation can be observed between OH-GQDs and t-GQDs, where the peak for t-GQDs shifts towards lower degrees, indicating a wider interlayer spacing. Moreover, the broadness of the observed peaks confirms the formation of GQDs with small sizes. Additionally, another peak is identified at approximately 31.80 degrees, corresponding to 100 hexagonal carbon planes. A distinct diffraction peak at an interlayer spacing of $2\theta = 5.59$ indicates the attachment of amine groups to the GQD plane [30].

The UV-visible absorption and emission spectra of t-GQDs and OH-GQDs are depicted in Fig. 5. It is worth noting that GQDs synthesized using different methods display distinct ultraviolet-visible absorption properties. Typically, the absorption peak associated with the $\pi \rightarrow \pi*$ transition falls within the $200 - 270$ nm wavelength range, indicating the changes of aromatic C=C bonds in the sp^2 hybridization region. On the other hand, the absorption peak related to the $n \rightarrow \pi*$ transition is observed above 260 nm, and it signifies the presence of C-O bonds. Through functionalization, the absorption peak at 250 nm of t-GQDs shifts to 230 nm, while the absorption peak at 350 nm shifts to

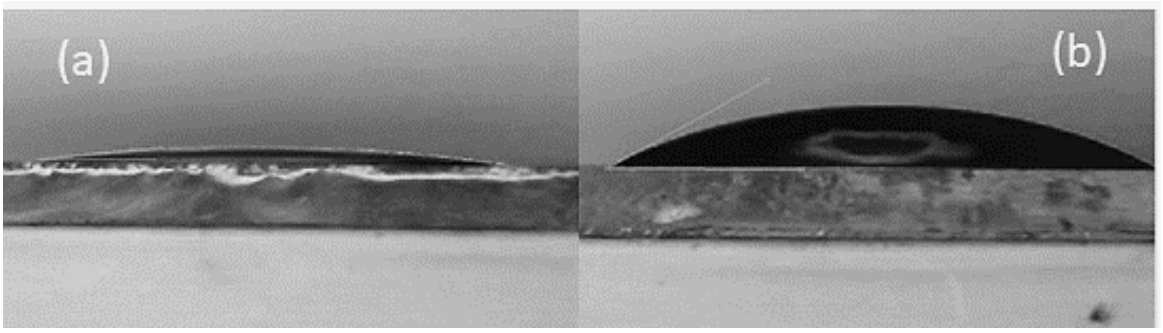

Figure 2. The contact angle measurement of (a) GQDs and (b) functionalized t-GQDs.

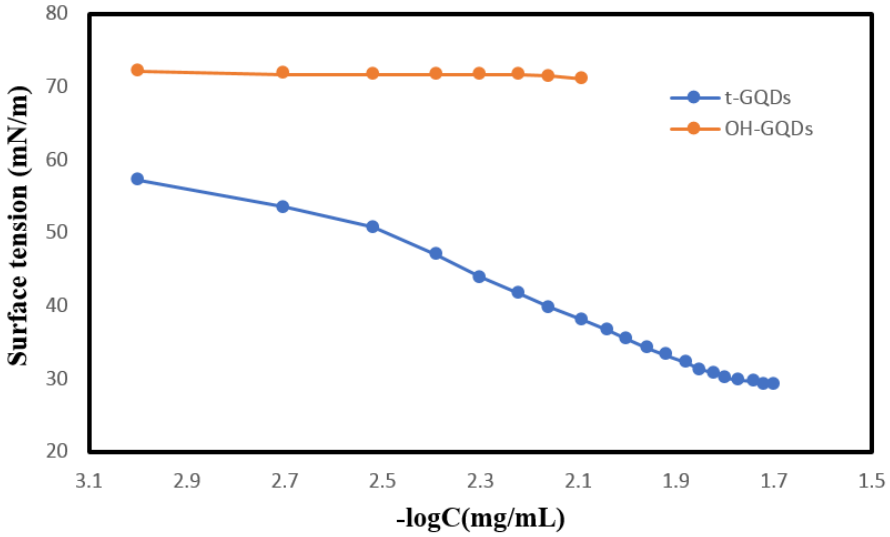

Figure 3. Surface tensions of aqueous dispersions of OH-GQDs and t-GQDs at various concentrations, measured using the ring method at 25 °C. The reduction in surface tension by t-GQDs (to 57.27 mN/m) compared to OH-GQDs (minimal reduction from water) demonstrates the amphiphilic character of the functionalized quantum dots.

290 nm. Fig. 5 (b) highlights that the maximum emission of OH-GQDs occurs at 610 nm, whereas t-GQDs exhibit maximum emissions at approximately 592 nm. Notably, amphiphilic GQDs experience blue shifts due to covalent interactions with hexylamine, leading to the reduction of carboxyl groups and surface passivation [31].

The surface charge of GQDs was assessed through zeta potential analysis. The presence of surface oxygen functionalities led to a notably negative zeta potential scattering for OH-GQDs (−46.4). However, upon functionalization with Tridecylamine, the surface charge of t-GQDs became less negative (−29.3), indicating a reduction in oxygenated functional groups [32]. For particle size determination, TEM analysis was conducted. Fig. 6 illustrates a distribution of OH-GQD sizes, with an average diameter of 2.38 nm. Estimating the particle size of t-GQDs, which accumulated after functionalization, proved challenging.

Nevertheless, SEM images were employed for particle size measurement. In general, t-GQDs exhibited a diameter of 18 nm. Utilizing SEM, the surface morphology of nanoparticles was predicted. Fig. 6 showcases SEM images of OH-GQDs and t-GQDs. Analysis of the SEM images confirmed the production of t-GQDs with a diameter of 24 nm, which is consistent with the observations in TEM images.

Aqueous graphite dispersions were prepared by exfoliating pristine graphite using various GQDs (t-GQDs1-4) and different ultrasound durations, producing graphene nanosheets in suspension. Ultrasonic force is a well-known external factor that enables the exfoliation of graphite through liquid phase exfoliation (LPE). Additionally, ultrasonication helps prevent the aggregation of graphene. To evaluate the dispersibility of different GQDs, the preparation process for all GQDs was conducted under identical conditions. The dispersion efficacy of each GQD was determined by measuring its UV-vis spectra. Our findings indicated variations in absorption intensities among graphene dispersions achieved

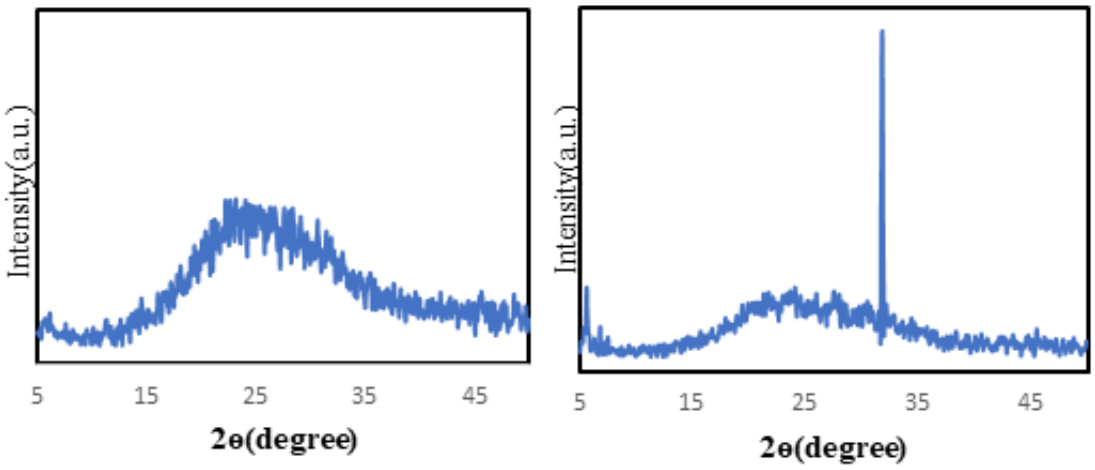

Figure 4. XRD pattern of a) OH- GQDs b) t-GQDs.

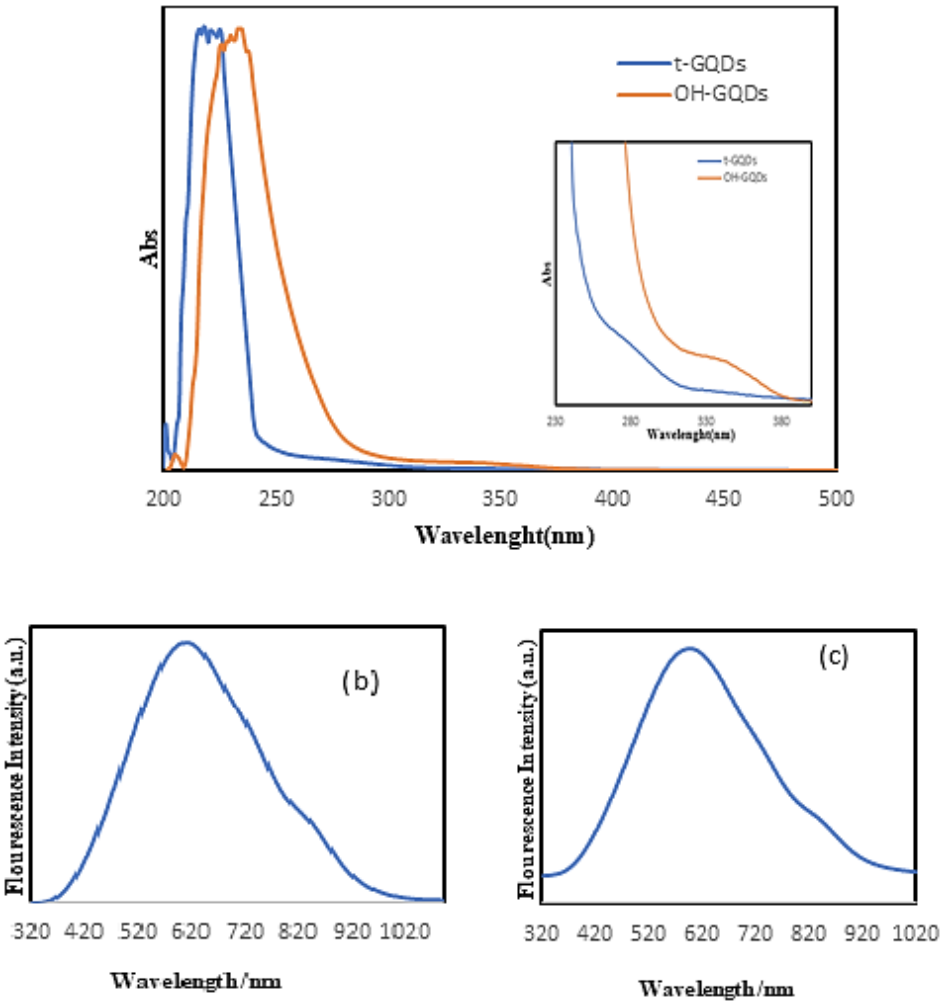

Figure 5. (a) UV-vis extinction spectra of the OH-GQDs and t-GQDs showing characteristic absorption bands. (b) Photoluminescence (PL) spectra of OH-GQDs excited at 360 nm. (c) PL spectra of t-GQDs excited at 360 nm. All spectra were corrected for light scattering using appropriate baseline subtraction. The absorption peaks at $230-250$ nm correspond to $\pi \rightarrow \pi^*$ transitions of aromatic C=C bonds, while peaks at $290-350$ nm are attributed to $n \rightarrow \pi^*$ transitions of C=O bonds.

through different GQDs. According to the Beer-Lambert law, the UV-vis spectrum's absorption intensity is directly linked to graphene concentration. It is worth noting that graphene dispersions and individual layers exhibit varying concentrations under different exfoliation conditions. Several parameters may be modified to attain the most desirable outcomes, including the duration of sonication, rotational speed during centrifugation, concentration, type of surfactant, and the initial concentration of graphite.

3.1 The effect of t-GQD concentration on graphene dispersion

The initial investigation focused on assessing the impact of different concentrations of t-GQDs on the quantity and quality of dispersed graphene under identical conditions. Fig. 7 presents the absorption spectrum of graphene solutions at varying concentrations (0.01, 0.04, 0.08, 0.12, 0.16, 0.20, 0.26 mg/mL) of t-GQDs1, t-GQDs2, t-GQDs3, and t-GQDs4, revealing a noticeable peak in UV-visible absorbance around 266 nm for all spectra. This peak in graphene's absorption spectrum is attributed to the $\pi \rightarrow \pi*$ transition of polyaromatic systems. The data from Fig. 7 demonstrates that the UV absorption of graphene consistently increases with a rise in t-GQD concentration. This observation is because the higher surfactant concentration allows for more significant adsorption of surfactant monomers onto the surface of graphene [33]. Consequently, graphene becomes progressively coated with t-GQDs, reducing the van der Waals interaction between graphene sheets and improving their dispersion.

Based on our analysis of the UV-vis spectra, we found that t-GQDs2 displayed 2.3 times higher UV absorbency compared to t-GQDs1 when dispersed in graphene using different surfactants at varying concentrations. Additionally, t-GQDs3 demonstrated 1.5 times greater absorption than t-GQDs2, while t-GQDs4 exhibited 1.05 times greater absorption than t-GQDs3. These findings corroborate the notion that the composition and quantity of functional groups play a significant role in influencing graphene properties. Moreover, we determined that the optimal concentration of t-GQDs4 for effectively dispersing graphene is 0.08 mg/mL. Notably, an increase in amine concentration positively impacts the yield of graphene. The surfactant developed by our team consists of planar aromatic structures with varying

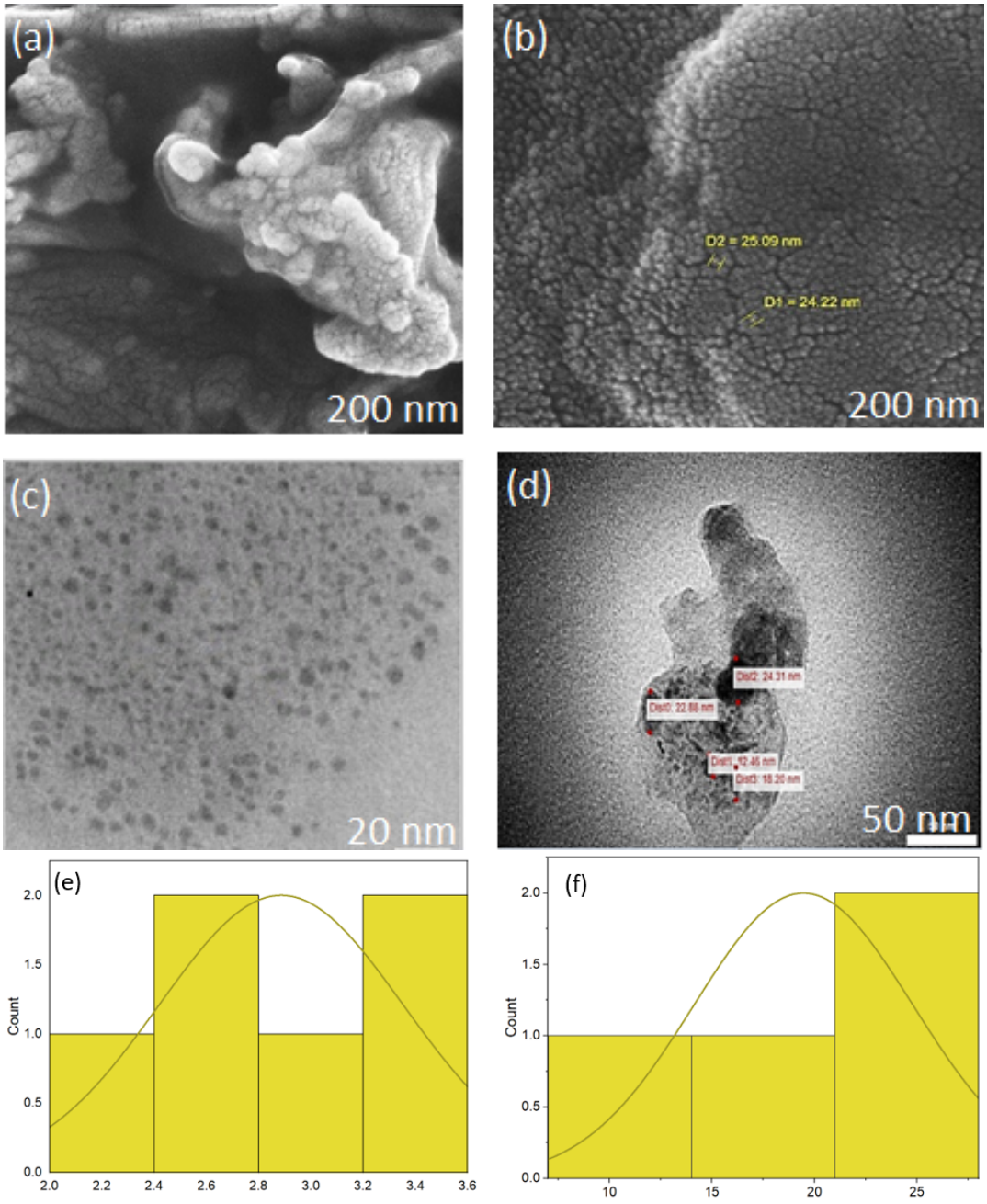

Figure 6. (a) SEM images of OH-GQDs (b) t-GQDs. (c) TEM images of OH-GQDs (d) t-GQDs. Size distribution histograms of (e) OH-GQDs (mean diameter $= 2.4 \pm 0.3$ nm, $n = 200$) and (f) t-GQDs (mean diameter $= 18 \pm 2$ nm, $n = 150$). ImageJ software obtained Size distributions by measuring individual particles from multiple TEM/SEM images.

quantities of alkyl chains (hydrophobic) and oxygen functional groups (hydrophilic). The hydrophobic group adheres to the graphite surface through $\pi - \pi$ interaction, while the hydrophilic group aligns itself towards water. During ionization in water, the negative charge provided the t-GQDs with excellent dispersibility due to their strong electrostatic repulsion, which overcomes van der Waals forces. Graphene powder, on the other hand, contained a lower proportion of oxygen-containing groups. As a result, they cannot generate sufficient surface charges to repel one another.

It is important to note that the term 'graphene powder' in our discussion refers to the dried product obtained after the graphite dispersions' exfoliation, purification, and filtration. This powder consists predominantly of few-layer graphene nanosheets, as confirmed by our Raman analysis. For UV-vis measurements of highly concentrated dispersions, appropriate dilutions were performed to ensure measurements remained in the linear response range of the spectrophotometer, with extinction values below 1.0. All reported concentration values have been corrected for these dilution factors.

Based on our analysis of the UV-vis spectra, we found that t-GQDs2 displayed 2.3 times higher UV absorbency compared to t-GQDs1 when dispersed in graphene using different surfactants at varying concentrations. Additionally, t-GQDs3 demonstrated 1.5 times greater absorption than t-GQDs2, while t-GQDs4 exhibited 1.05 times greater absorption than t-GQDs3. These findings corroborate the no-

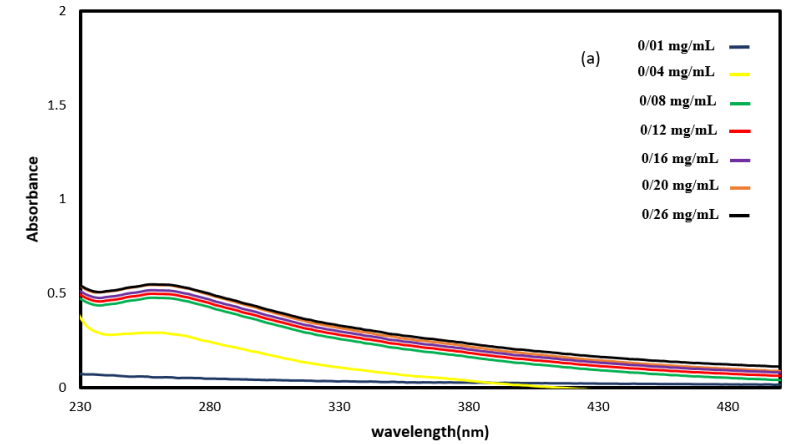
(a)
0/01 mg/mL
0/04 mg/mL
0/08 mg/mL
0/12 mg/mL
0/16 mg/mL
0/20 mg/mL
0/26 mg/mL
Absorbance
wavelength(nm)

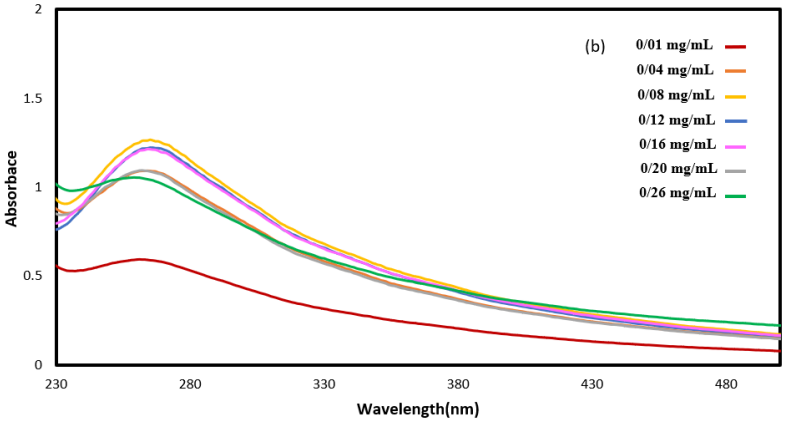
(b)
0/01 mg/mL
0/04 mg/mL
0/08 mg/mL
0/12 mg/mL
0/16 mg/mL
0/20 mg/mL
0/26 mg/mL
Absorbace
Wavelength(nm)

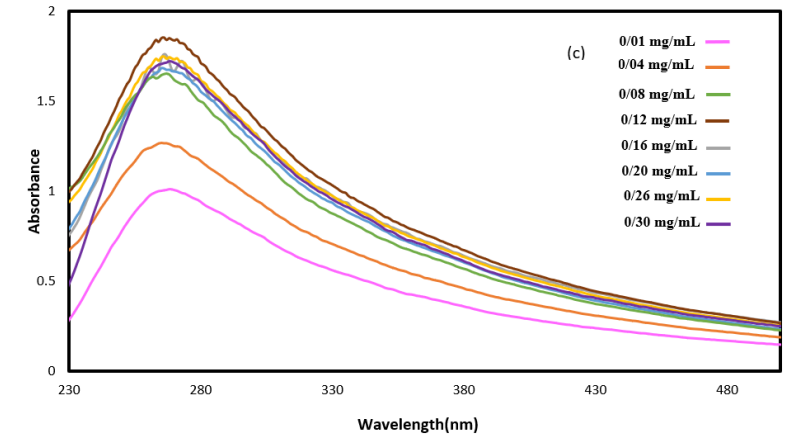
(c)
0/01 mg/mL
0/04 mg/mL
0/08 mg/mL
0/12 mg/mL
0/16 mg/mL
0/20 mg/mL
0/26 mg/mL
0/30 mg/mL
Absorbance
Wavelength(nm)

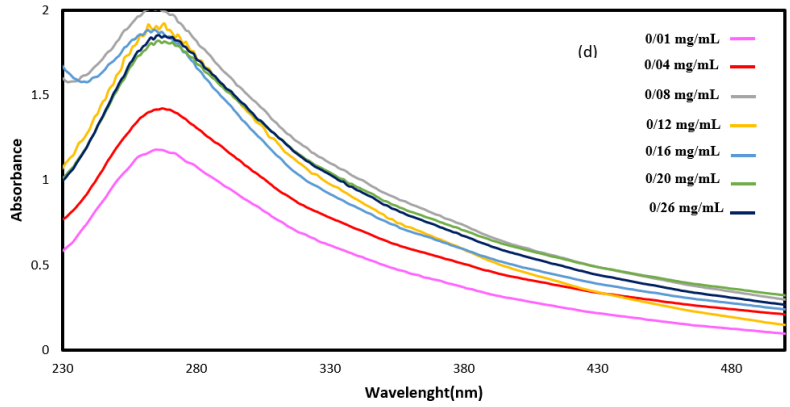
(d)
0/01 mg/mL
0/04 mg/mL
0/08 mg/mL
0/12 mg/mL
0/16 mg/mL
0/20 mg/mL
0/26 mg/mL
Absorbance
Wavelenght(nm)

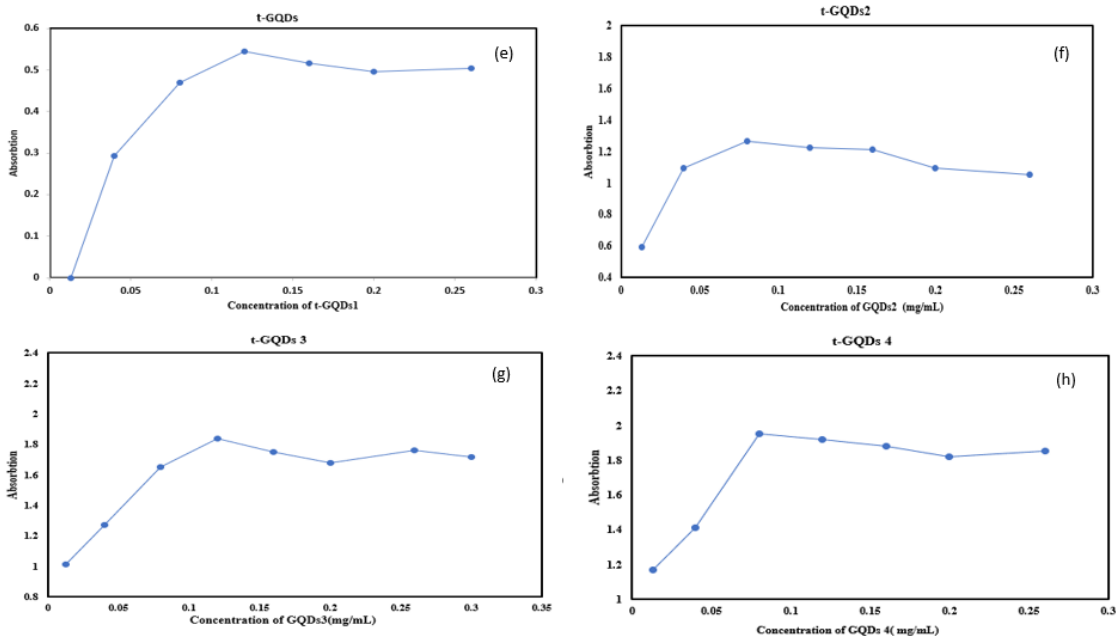

Figure 7. UV-vis extinction spectra of exfoliated graphite dispersions at different concentrations of surfactant: (a) t-GQDs1, (b) t-GQDs2, (c) t-GQDs3, (d) t-GQDs4. Samples were diluted when extinction values approached 1.0 to ensure measurements remained in the linear range. Dilution factors were applied to calculate actual concentration values.

tion that the composition and quantity of functional groups play a significant role in influencing graphene properties. Moreover, we determined that the optimal concentration of t-GQDs4 for effectively dispersing graphene is 0.08 mg/mL. Notably, an increase in amine concentration positively impacts the yield of graphene. The surfactant developed by our team consists of planar aromatic structures with varying quantities of alkyl chains (hydrophobic) and oxygen functional groups (hydrophilic). The hydrophobic group adheres to the graphite surface through $\pi - \pi$ interaction, while the hydrophilic group aligns itself towards water. During ionization in water, the negative charge provided the t-GQDs with excellent dispersibility due to their strong electrostatic repulsion, which overcomes van der Waals forces. Graphene powder, on the other hand, contained a lower proportion of oxygen-containing groups. As a result, they cannot generate sufficient surface charges to repel one another.

3.2 The effect of ultrasonic time on graphene dispersion

To explore the ideal conditions for dispersing graphene, we utilized variations in ultrasonic time to investigate this phenomenon. A series of experiments ranging from 15 minutes to 120 minutes of sonication time were performed for this purpose. Analyzing Fig. 5 (d) shows that t-GQDs4 displays the most notable concentration in dispersing. Furthermore, when the t-GQD4 concentration is maintained at 0.08 mg/mL, the exfoliation yield gradually escalates as the sonication time is extended from 15 to 90 minutes before reaching a stable state (Fig. 8).

Fig. 8 illustrates the UV-vis spectra of graphene dispersions with varying ultrasonic times of t-GQD4. However, it is essential to note that absorption values close to 2 indicate that the limit of 0% transmittance has been reached, leading to potential saturation of the signal. Therefore, the information concerning the increase in concentration may be distorted beyond this point and should be interpreted cautiously.

The stability of graphene dispersions was assessed using zeta potentials. In an aqueous solution, GQDs absorb onto a graphene surface. Due to the GQD absorption, the local graphene domain became negatively charged. It was found that the zeta potential of the graphene dispersion was measured to be -40.5 mV, significantly lower than the accepted value of -25 mV, which ensures colloidal stability. This indicates that the graphene was effectively dispersed in water without aggregation. To evaluate the quality of graphene and the level of defects, Raman spectroscopy was employed by excitation wavelength 532 nm. A Raman spectrum of graphene typically exhibits three main features: G (1580 cm^{-1}), D (1350 cm^{-1}), and 2D (2720 cm^{-1}) peaks, each representing distinct characteristics. The D band signifies the presence of defects, and the ID/IG intensity ratio quantifies the extent of these defects. A lower ratio value implies a superior quality of the graphene's crystalline structure, demonstrating higher perfection. The ID/IG ratio of our graphene specimen is below 0.23. Estimating the number of graphene layers can be achieved by analyzing 2D peaks in the Raman spectrum, an accepted method. Previous studies [34, 35] have shown that as the G peak-to-2D peak intensity ratio (IG/I2D) increases, the number of graphene layers also increases. For instance, bilayer graphene has IG/I2D values ranging from 2.2 to 3.5, while trilayer graphene has values ranging from 3.5 to 4.5. By referring to Fig. 9, it is evident that the IG/I2D ratio of the dispersed graphene using t-GQD is lower than 3.5, suggesting the presence of $2-3$ graphene layers.

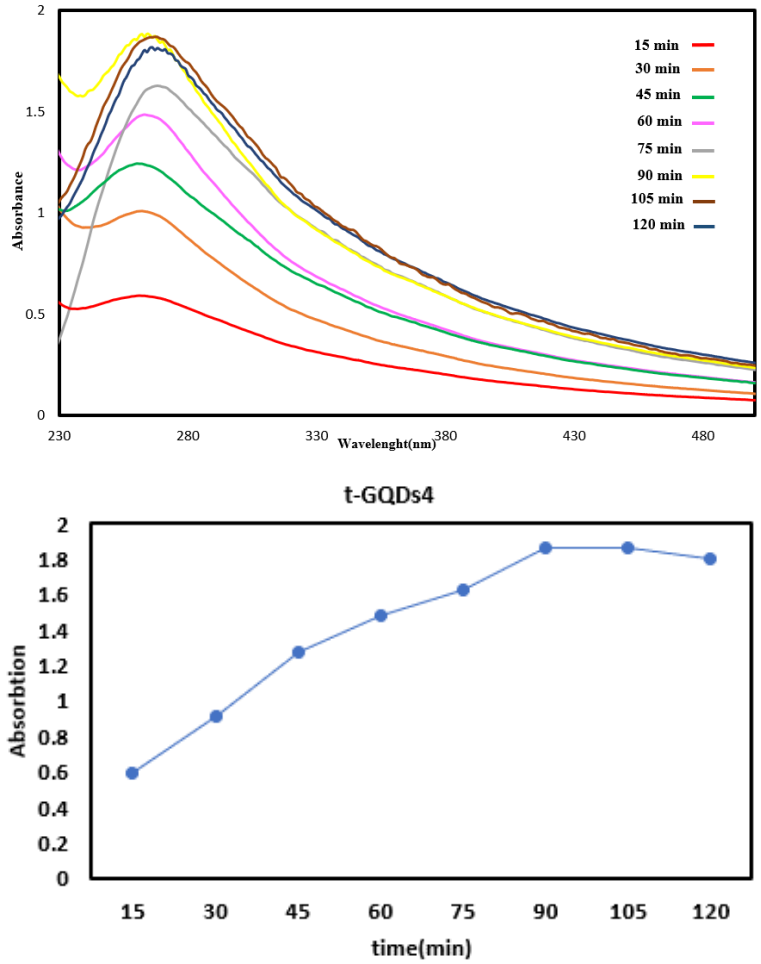

Figure 8. UV-vis spectra of graphene dispersions with different ultrasonic times of t-GQD4. Note that absorption values approaching 2 indicate that signal saturation has been reached, and thus, the concentrations beyond this point may lead to distorted information regarding the concentration effects. Care should be taken when interpreting data at higher concentrations.

3.3 Interaction mechanism between amphiphilic GQDs and graphite

The exceptional performance of t-GQDs in exfoliating and stabilizing graphene can be attributed to the unique interaction mechanisms between the amphiphilic GQDs and graphite surfaces. This interaction involves synergistic forces working to overcome the strong van der Waals attraction between graphene layers. The stabilization mechanism of tridecylamine-functionalized GQDs (t-GQDs) primarily involves two key interactions: van der Waals forces and steric repulsion. The $\pi - \pi$ interactions between the aromatic rings of t-GQDs and the graphene sheets facilitate

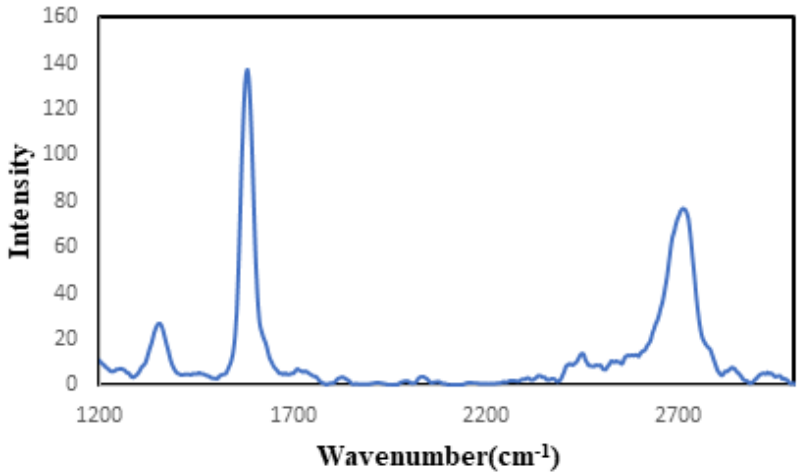

Figure 9. Raman spectroscopy of graphene.

strong adhesion, preventing the sheets from aggregating. Additionally, the hydrophobic tridecyl chains extend into the surrounding solvent, creating a steric barrier that further inhibits the reaggregation of graphene layers. This strong adsorption and steric hindrance combination ensures a stable dispersion of graphene in aqueous media.

The primary interaction mechanism relies on the $\pi - \pi$ stacking between the aromatic domains of t-GQDs and the sp^2 hybridized carbon network of graphite. The planar aromatic structure of the GQD core allows for effective parallel alignment with graphene sheets, maximizing orbital overlap and facilitating strong non-covalent binding. This $\pi - \pi$ interaction is significantly stronger than the simple hydrophobic interactions observed with conventional surfactants, explaining the superior performance of t-GQDs in graphene exfoliation.

The hydrophobic tridecylamine chains in t-GQDs also play a crucial role in exfoliation. These chains preferentially interact with the hydrophobic graphene surface through van der Waals forces and hydrophobic effects. Our experimental results demonstrate that increasing the amine content (from t-GQDs1 to t-GQDs4) enhances graphene dispersion yield, confirming the importance of these hydrophobic interactions. The optimal performance observed with t-GQDs4 can be attributed to the ideal balance between hydrophobic and hydrophilic components, which maximizes graphene binding strength and aqueous solubility.

The hydrophilic carboxyl and hydroxyl groups on t-GQDs extend into the aqueous medium, creating electrostatic and steric barriers against reaggregation. The negative charges on these groups (confirmed by zeta potential measurements of -40.5 mV) generate strong electrostatic repulsion between graphene sheets coated with t-GQDs. This dual stabilization mechanism combining strong $\pi - \pi$ binding with electrostatic repulsion explains the exceptional stability of our graphene dispersions compared to those prepared with conventional surfactants.

Furthermore, the amphiphilic nature of t-GQDs allows them to effectively reduce the interfacial tension between the hydrophobic graphene surface and water, as evidenced by our surface tension measurements (Fig. 3). This interfacial activity facilitates the exfoliation process by reducing the energy barrier for separating graphene layers in aqueous media.

The concentration-dependent behavior observed in our experiments (Fig. 7) suggests a progressive adsorption mechanism, where t-GQDs initially adsorb onto accessible graphite surfaces, weakening interlayer interactions and facilitating further exfoliation through sonication. As the concentration of t-GQDs increases, more complete surface coverage is achieved, enhancing the stability of exfoliated graphene sheets through increased electrostatic and steric repulsion.

4. Conclusion

In essence, our study has successfully demonstrated the effectiveness of amphiphilic GQDs as a novel surfactant for graphene dispersion, exhibiting significant advantages over conventional dispersants. Through a straightforward bottom-up synthesis method, we have successfully modified OH-GQDs by incorporating hydrophobic Tridecylamine, resulting in amphiphilic GQDs with a unique dual-stabilization mechanism.

The superior performance of t-GQDs compared to conventional surfactants (SDS) and non-amphiphilic GQDs can be attributed to their distinctive dual-stabilization mechanism:

1) **$\pi - \pi$ interactions**: The conjugated aromatic rings in the basal plane of these GQDs facilitate strong adsorption onto the graphite surface through $\pi - \pi$ interactions, which conventional surfactants like SDS cannot provide. This strong adsorption prevents the reaggregation of graphene sheets more effectively than electrostatic stabilization alone.

2) **Steric and electrostatic stabilization**: The hydrophilic functional groups (carboxyl/hydroxyl) extend into the aqueous phase, providing electrostatic repulsion between graphene sheets and steric barriers against reaggregation. The negative charge (confirmed by zeta potential measurements of -40.5 mV) ensures exceptional colloidal stability through strong electrostatic repulsion.

3) **Amphiphilic balance**: The optimized ratio of hydrophobic tridecylamine to hydrophilic groups in t-GQDs4 provides the ideal balance for maximum graphene dispersion, yielding up to 2.7 times higher graphene concentration than conventional methods.

Our comparative analysis demonstrated that t-GQDs disperse a significantly higher graphene concentration (1.9 times more than SDS) with substantially improved long-term stability (only a 12% reduction in concentration after 30 days compared to 45% for SDS). These findings establish amphiphilic GQDs as a superior alternative to traditional dispersants for graphene exfoliation and stabilization in aqueous media. This research provides a foundation for developing more efficient graphene processing methods using custom-designed amphiphilic GQDs, potentially enabling industrial-scale production of high-quality graphene dispersions for various applications.

The significance of this study lies in its demonstration of a simple, scalable approach to producing amphiphilic GQDs that significantly outperform conventional surfactants for graphene production. Unlike previous methods requiring complex functionalization procedures, our one-pot hydrothermal synthesis provides an environmentally friendly and economically viable pathway to produce efficient graphene dispersants. The superior performance of t-GQDs in exfoliating graphite represents an important advancement toward industrial-scale production of high-quality graphene dispersions. The insights gained regarding the structural features that enhance dispersing efficiency could inform the rational design of next-generation carbon nanomaterial dispersants. Furthermore, the amphiphilic GQDs developed here may find applications beyond graphene production, including stabilizers for other nanomaterials, interfacial agents in composite materials, or multifunctional platforms for sensing and bioimaging applications.

Acknowledgement
The Iran University of Science and Technology has supported this work greatly. Therefore, we want to thank them absolutely for all their help.

Authors Contribution
Zahra Azimi: Writing, Methodology, review & editing. Beheshteh Sohrabi: Supervision, conceptualization, Methodology. Yasaman Javanmard: Investigation. Armin Hajipour Keyhani: review & editing.

Availability of data and materials
The data supporting this study's findings are available from Y. J., but restrictions apply to the availability of these data, which were used under license for the current study and are not publicly available. Data are, however, available from the authors upon reasonable request and with permission from B. S.

Conflict of interests
The author states that there is no conflict of interest.

References

[1] L. Zhao, W. Liu, W. Yi, T. Hu, D. Khodagholian, F. Gu, H. Lin, E. Zurek, Y. Zheng, and M. Miao. "Nano-makisu: highly anisotropic two-dimensional carbon allotropes made by weaving together nanotubes". *Nanoscale*, **12**:347–355, 2020.
DOI: https://doi.org/10.1039/c9nr08069d.

[2] K.S. Novoselov, A.K. Geim, S.V. Morozov, D. Jiang, Y. Zhang, S.V. Dubonos, I.V. Grigorieva, and A.A. Firsov. "Electric field in atomically thin carbon films". *Science*, **306**:666–669, 2004.
DOI: https://doi.org/10.1126/science.1102896.

[3] H. Yang, F. Bao, S. Chen, S. Liu, H. Huang, L. Wang, H. Liu, J. Yu, C. Zhu, and J. Xu. "Construction of a Borophene-Based Hybrid Aerogel for Multifunctional Applications". *ACS Appl. Mater. Interfaces.*, **16**:56063–56072, 2024.
DOI: https://doi.org/10.1021/acsami.4c10663.

[4] T. Wei, F. Hauke, and A. Hirsch. "Evolution of Graphene Patterning: From Dimension Regulation to Molecular Engineering". *Adv. Mater.*, **33**:e2104060, 2021.
DOI: https://doi.org/10.1002/adma.202104060.

[5] R. Narayan and S.O. Kim. "Surfactant mediated liquid phase exfoliation of graphene ". *Nano Converg*, **2**:20, 2015.
DOI: https://doi.org/10.1186/s40580-015-0050-x.

[6] J. Fernandes, S.S. Nemala, G. De Bellis, and A. Capasso. "Green Solvents for the Liquid Phase Exfoliation Production of Graphene: The Promising Case of Cyrene". *Front. Chem.*, **10**:878799, 2022.
DOI: https://doi.org/10.3389/fchem.2022.878799.

[7] S. Calistri, A. Ubaldini, C. Telloli, F. Gennerini, G. Marghella, A. Gessi, S. Bruni, and A. Rizzo. "Exfoliation of Molecular Solids by the Synergy of Ultrasound and Use of Surfactants: A Novel Method Applied to Boric Acid". *Molecules*, **29**, 2024.
DOI: https://doi.org/10.3390/molecules29143324.

[8] W. Zhao, A. Sugunan, T. Gillgren, J.A. Larsson, Z.-B. Zhang, S.-L. Zhang, N. Nordgren, J. Sommertune, and A. Ahniyaz. "Surfactant-Free Stabilization of Aqueous Graphene Dispersions Using Starch as a Dispersing Agent". *ACS Omega*, **6**:12050–12062, 2021.
DOI: https://doi.org/10.1021/acsomega.1c00699.

[9] H.-H. Cho, H. Yang, D.J. Kang, and B.J. Kim. "Surface engineering of graphene quantum dots and their applications as efficient surfactants". *ACS Appl. Mater. Interfaces.*, **7**:8615–8621, 2025.
DOI: https://doi.org/10.1021/acsami.5b00729.

[10] B. Kuehl, S. Raman, A. Becker, V. Garg, J. Roberts-Dobie, A. McCaslin, J. Brensdal, J. Attinger, L. Burton, M. Forrester, A. Hohmann, and E.W. Cochran. "Fully Atom-Efficient Solvent-Mediated Biopolymer Manufacturing: A Base Case Illustrated with Macromolecular Surfactants Tailored to Stable Polymer-Water Interfaces". *ACS Appl. Mater. Interfaces.*, **16**:59280–59290, 2024.
DOI: https://doi.org/10.1021/acsami.4c12730.

[11] A. Griffin, K. Nisi, J. Pepper, A. Harvey, B.M. Szydłowska, J.N. Coleman, and C. Backes. "Effect of Surfactant Choice and Concentration on the Dimensions and Yield of Liquid-Phase-Exfoliated Nanosheets". *Chem. Mater.*, **32**:2852–2862, 2020.
DOI: https://doi.org/10.1021/acs.chemmater.9b04684.

[12] A. Gotzias and Y.G. Lazarou. "Graphene Exfoliation in Binary NMP/Water Mixtures by Molecular Dynamics Simulations". *Chempluschem*, **89**:e202300758, 2024.
DOI: https://doi.org/10.1002/cplu.202300758.

[13] Y.-C. Hung, J.-R. Wu, A.P. Periasamy, N. Aoki, and C. Chuang. "Advances in spin properties of plant leaf-derived graphene quantum dots from materials to applications". *Nanotechnology*, **36**, 2025.
DOI: https://doi.org/10.1088/1361-6528/adb851.

[14] C. Zhao, X. Song, Y. Liu, Y. Fu, L. Ye, N. Wang, F. Wang, L. Li, M. Mohammadniaei, M. Zhang, Q. Zhang, and J. Liu. "Synthesis of graphene quantum dots and their applications in drug delivery". *J Nanobiotechnol*, **18**:142, 2020.
DOI: https://doi.org/10.1186/s12951-020-00698-z.

[15] J.P. Naik, P. Sutradhar, and M. Saha. "Molecular scale rapid synthesis of graphene quantum dots (GQDs)". *J Nanostruct Chem*, **7**:85–89, 2017.
DOI: https://doi.org/10.1007/s40097-017-0222-9.

[16] N. Manjubaashini, T.D. Thangadurai, D. Nataraj, and S. Thomas. "Introduction to Graphene Quantum Dots. Materials Horizons: From Nature to Nanomaterials". Book Chapter Springer:27–41, 2024.
DOI: https://doi.org/10.1007/978-981-97-5722-0_3.

[17] V. Dananjaya, S. Marimuthu, R. Yang, A.N. Grace, and C. Abeykoon. "Synthesis, properties, applications, 3D printing and machine learning of graphene quantum dots in polymer nanocomposites". *Progress in Materials Science*, **144**:101282, 2024.
DOI: https://doi.org/10.1016/j.pmatsci.2024.101282.

[18] Z. Xie, R. Lu, Y. Zhu, M. Peng, T. Fan, P. Ren, B. Wang, L. Kang, X. Liu, S. Li, and H. Cui. "Liquid-phase exfoliation of black sesame to create a nanoplatform for in vitro photoluminescence and photothermal therapy". *Nanomedicine (Lond).*, **15**:2041–2052, 2020.
DOI: https://doi.org/10.2217/nnm-2020-0151.

[19] Z. Azimi, M. Alimohammadian, and B. Sohrabi. "Graphene Quantum Dots Based on Mechanical Exfoliation Methods: A Simple and Eco-Friendly Technique". *ACS Omega.*, **9**:31427–31437, 2024.
DOI: https://doi.org/10.1021/acsomega.4c00453.

[20] R. Ma, M. Zeng, D. Huang, J. Wang, Z. Cheng, and Q. Wang. "Amphiphilicity-adaptable graphene quantum dots to stabilize pH-responsive pickering emulsions at a very low concentration". *J. Colloid Interface Sci.*, **601**:106–113, 2021.
DOI: https://doi.org/10.1016/j.jcis.2021.05.104.

[21] Q. Zhou, G. Xia, M. Du, Y. Lu, and H. Xu. "Scotch-tape-like exfoliation effect of graphene quantum dots for efficient preparation of graphene nanosheets in water". *Appl. Surf. Sci.*, **483**, 2019.
DOI: https://doi.org/10.1016/j.apsusc.2019.03.290.

[22] A. Hadi, J. Zahirifar, J. Karimi-Sabet, and A. Dastbaz. "Graphene nanosheets preparation using magnetic nanoparticle assisted liquid phase exfoliation of graphite: The coupled effect of ultrasound and wedging nanoparticles". *Ultrason. Sonochem*, **44**:204–214, 2018.
DOI: https://doi.org/10.1016/j.ultsonch.2018.02.028.

[23] Z. Ke, M. Azam, S. Ali, M. Zubair, Y. Cao, A.A. Khan, A. Hassan, and W. Xue. "Role of Functional Groups in Tuning Luminescence Signature of Solution-Processed Graphene Quantum Dots: Experimental and Theoretical Insights". *Molecules*, **29**, 2024.
DOI: https://doi.org/10.3390/molecules29122790.

[24] D. Pan, J. Zhang, Z. Li, and M. Wu. "Hydrothermal Route for Cutting Graphene Sheets into Blue-Luminescent Graphene Quantum Dots". *Advanced Materials*, **22**:734–738, 2010.
DOI: https://doi.org/10.1002/adma.200902825.

[25] M. Cai, L. Lai, and M. Zhao. "Synthesis, properties, and applications of amphiphilic carbon dots: A review". *Carbon*, **233**:119921, 2025.
DOI: https://doi.org/10.1016/j.carbon.2024.119921.

[26] F. Xi, J. Zhao, C. Shen, J. He, J. Chen, Y. Yan, K. Li, J. Liu, and P. Chen. "Amphiphilic graphene quantum dots as a new class of surfactants". *Carbon*, **153**:127–135, 2019.
DOI: https://doi.org/10.1016/j.carbon.2019.07.014.

[27] Y. Dong, J. Shao, C. Chen, H. Li, R. Wang, Y. Chi, X. Lin, and G. Chen. "Blue luminescent graphene quantum dots and graphene oxide prepared by tuning the carbonization degree of citric acid". *Carbon N. Y.*, **50**:4738–4743, 2012.
DOI: https://doi.org/10.1016/J.CARBON.2012.06.002.

[28] N. Saito, S. Itoyama, R. Takahashi, Y. Takahashi, and Y. Kondo. "Synthesis and surface activity of photoresponsive hybrid surfactants containing both fluorocarbon and hydrocarbon chains". *J. Colloid Interface Sci.*, **582**:638–646, 2021.
DOI: https://doi.org/10.1016/j.jcis.2020.08.054.

[29] S. Kapoor, A. Jha, H. Ahmad, and S.S. Islam. "Avenue to Large-Scale Production of Graphene Quantum Dots from High-Purity Graphene Sheets Using Laboratory-Grade Graphite Electrodes". *ACS Omega.*, **5**:18831–18841, 2020.
DOI: https://doi.org/10.1021/acsomega.0c01993.

[30] P. Singh, H. Vithalani, A. Adhyapak, T. Semwa, N. Singh, M. Dhanka, D. Bhatia, and J. Saha. "Microwave-Assisted Green Synthesis of Fluorescent Graphene Quantum Dots: Metal Sensing, Antioxidant Properties, and Biocompatibility Insights". *J. Fluoresc*, **35**, 2025.
DOI: https://doi.org/10.1007/s10895-025-04140-1.

[31] W. Zhang, Y. Liu, X. Meng, T. Ding, Y. Xu, H. Xu, Y. Ren, B. Liu, J. Huang, J. Yang, and X. Fang. "Graphenol defects induced blue emission enhancement in chemically reduced graphene quantum dots". *Phys. Chem. Chem. Phys.*, **17**:22361–22366, 2015.
DOI: https://doi.org/10.1039/c5cp03434e.

[32] A.A. Bhosle, M. Banerjee, S.D. Hiremath, D.S. Sisodiya, V.G. Naik, N. Barooah, A.C. Bhasikuttan, A. Chattopadhyay, and A. Chatterjee. "A combination of a graphene quantum dots-cationic red dye donor-acceptor pair and cucurbituril as a supramolecular sensor for ultrasensitive detection of cancer biomarkers spermine and spermidine". *J. Mater. Chem. B.*, **10**:8258–8273, 2022.
DOI: https://doi.org/10.1039/d2tb01269c.

[33] L. Golubewa, T. Kulahava, A. Klimovich, D. Rutkauskas, I. Matulaitiene, R. Karpicz, N. Belko, D. Mogilevtsev, A. Kavalenka, M. Fetisova, P. Karvinen, Y. Svirko, and P. Kuzhir. "Visualizing hypochlorous acid production by human neutrophils with fluorescent graphene quantum dots". *Nanotechnology*, **33**, 2021.
DOI: https://doi.org/10.1088/1361-6528/ac3ce4.

[34] J. Wang, K.K. Manga, Q. Bao, and K.P. Loh. "High-Yield Synthesis of Few-Layer Graphene Flakes through Electrochemical Expansion of Graphite in Propylene Carbonate Electrolyte". *J. Am. Chem. Soc.*, **133**:8888–8891, 2011.
DOI: https://doi.org/10.1021/ja203725d.

[35] M.S. Kang, K.T. Kim, J.U. Lee, and W.H. Jo. "Direct exfoliation of graphite using a non-ionic polymer surfactant for fabrication of transparent and conductive graphene films". *J. Mater. Chem. C.*, **1**: 1870–1875, 2013.
DOI: https://doi.org/10.1039/C2TC00586G.